Temperature- and rate-dependent RHEED oscillation studies of epitaxial Fe(001) on Cr(001)

K. Theis-Bröhl, I. Zoller, P. Bödeker, T. Schmitte, and H. Zabel
Institut für Experimentalphysik/Festkörperphysik, Ruhr-Universität Bochum, D-44780 Bochum, Germany

L. Brendel, M. Belzer, and D. E. Wolf
Institut für Theoretische Physik, Gerhard-Mercator-Universität-GH-Duisburg, D-47048 Duisburg, Germany
(Received 10 June 1997; revised manuscript received 14 October 1997)

Reflection high-energy electron diffraction (RHEED) intensity studies were performed during the growth of thin Fe layers on vicinal Cr(001)/Nb(001)/$Al_2O_3(1\bar{1}02)$ substrates. The results are compared with those of recent molecular-beam epitaxy (MBE) growth models. General agreement is found as concerns the linear relationship between the logarithm of the number of RHEED oscillations and the inverse growth temperature. In agreement with theory the RHEED oscillation damping time is found to depend algebraically on the growth rate. However, contrary to expectations, the RHEED oscillations vanish faster at higher growth temperatures and lower growth rates. This behavior can be explained by a change in the growth mode from layer-by-layer to step flow. Numerical simulations in which step bunch melting during the Fe growth on the Cr buffer is assumed reproduce well the present experimental results. [S0163-1829(98)02708-8]

I. INTRODUCTION

In this paper we report the growth behavior of thin Fe layers on Cr(001)/Nb(001)/$Al_2O_3(1\bar{1}02)$ substrates as monitored by *in situ* reflection high-energy electron diffraction (RHEED) oscillations. The work was stimulated by the discussion about the effect of interlayer roughness on the magnetic coupling behavior in Fe/Cr(001) sandwich structures and superlattices. There is a clear need for a detailed knowledge about the growth behavior and its effect on interface morphology. The Fe/Cr(001) system is one of the most frequently investigated transition-metal systems as concerns the magnetic properties. As a function of the Cr layer thickness, it exhibits a long-range magnetic oscillatory exchange coupling,[1–3] superposed by a 2-ML oscillation coupling period.[4,5] Additionally, giant magnetoresistance (GMR) was discovered first in this system.[6,7]

The exchange coupling in all magnetic superlattices is strongly affected by interface roughness, which has also been confirmed theoretically.[8] In Fe/Cr this effect is particularly severe, because of the intrinsic antiferromagnetic structure of the Cr spacer layer. Thus, the short 2-ML oscillation period can only be observed in samples with reduced interface roughness, prepared, for instance, on Fe whiskers at elevated growth temperatures.[4,9,10] For nonperfect interfaces, the roughness leads to a noncollinear alignment of the magnetization vectors in adjacent Fe layers, first reported by Rührig *et al.*[11] These noncollinear magnetic structures are due to spin frustrations at steps on the Fe/Cr interface whenever odd and even numbers of Cr monolayers are encountered. Different models describing the effect of roughness on the exchange coupling were discussed by Slonczewski[12] and Fullerton *et al.*,[13] while calculations by Stoeffler and co-workers[14] indicate a strong suppression of the Cr moments at the interface, thus reducing the coupling strength and behavior. Experimental confirmation for the connection between interfacial roughness in Fe/Cr superlattices and noncollinear exchange coupling was recently derived from polarized neutron scattering studies.[15]

The standard *in situ* technique for studying epitaxial growth is reflection high-energy electron diffraction.[16] In this technique the sample surface is illuminated at grazing incidence by a high-energy electron beam (typically 10–50 keV). Due to the scattering geometry this method is sensitive to both surface structure and morphology. An oscillation of the RHEED specularly diffracted intensity was first observed during the molecular beam epitaxial (MBE) growth of GaAs (Refs. 17 and 18) and was later also seen in metal epitaxy.[19–21] RHEED oscillations from a periodically varying surface step density are generally considered to be a signature of layer-by-layer growth. The period of these oscillations is often found to correspond to the time needed for the deposition of 1 ML. Dynamic calculations of RHEED for GaAs growth imply a rapid decrease of the oscillation amplitude with increasing surface roughness.[22] Therefore, strongly damped or absent RHEED oscillations are connected to island or three-dimensional (3D) growth behavior and therefore imply higher surface roughness. However, for a step-flow growth mode in which growth starts at step edges, a lack of RHEED oscillations is explained by a stable and constant surface roughness.

RHEED intensity oscillations have also been used to confirm the surface quality of Fe/Cr(001). Very high surface quality of the growing film was reported by RHEED on Cr/Fe/Cr(001) trilayers grown on Fe whiskers[9] at a substrate temperature of 300 °C. The RHEED oscillations maintain almost the same intensity amplitude during the growth of several monolayers Cr(001) on the Fe whisker substrate, thus demonstrating extremely perfect layer-by-layer growth. A correlation between elevated substrate temperature and a reduced surface roughness as obtained in Fe/Cr(001) was also shown in growth studies of Fe on Fe whiskers.[23] As in the case of Fe/Cr on Fe whiskers, nearly perfect layer-by-layer growth is reached for growth at 250 °C. For Fe growth on Cu(001) Schatz *et al.*[24] found a similar temperature behavior.

Strong RHEED oscillations accompanying predominantly layer-by-layer growth behavior were found at slightly higher temperatures between 60 and 100 °C, compared to 3D growth for temperatures below room temperature.

II. SAMPLE PREPARATION

For growing Fe(001) epitaxially on Cr(001) a 3 in. RIBER metal MBE system (equipped with two electron beam hearths and three ports for effusion cells) was used; the MBE machine is described elsewhere.[25] One of the electron beam evaporators contains four rotable crucibles so that a total of 8 different materials can be evaporated from this system.

The substrates were $Al_2O_3(1\bar{1}02)$ crystals with surfaces of epitaxial grade finish. These were degreased by sonication in the standard fashion and annealed in UHV at 1000 °C for 1 h prior to growth. A buffer layer of 250 Å Nb(001) was first deposited with a substrate temperature of 900 °C. Nb was evaporated from one of the 14 cm^3 crucibles for e^--beam evaporation. Subsequently, the sample was annealed for 30 min at 950 °C to smooth the Nb surface. The growth behavior of Nb on different sapphire orientations is well documented.[26–30] Nb nucleates with respect to the sapphire in a so-called *three-dimensional epitaxial relationship* (3D-ER). This relationship explains a distinct geometrical arrangement of the bcc Nb unit cell to the hexagonal sapphire unit cell. According to the arrangement of both unit cells, a suitable sapphire substrate orientation can be found for growing a Nb layer in a distinct orientation. Both orientations are parallel or nearly parallel in the 3D-ER. It was found that Nb(110) grows epitaxially on $Al_2O_3(1120)$, Nb(111) on $Al_2O_3(0001)$, Nb(001) on $Al_2O_3(1102)$, and Nb(211) on $Al_2O_3(1100)$. Furthermore, relations between the individual crystal axes can be derived. In the case of Nb(110) and Nb(111) the distinct crystal planes of both materials are exactly parallel in the 3D-ER and epitaxial growth with a very high quality can be achieved.[26–28] However, Nb(001) is not exactly parallel to any of the low-index crystal sapphire planes in the 3D-ER. Instead, it is tilted by 2.8° towards the $Al_2O_3(1102)$ crystal plane. Nevertheless, epitaxial growth has also been found for this case in spite of the tilt. This was confirmed experimentally by Knowles *et al.*[31] and Di Nunzio, Theis-Bröhl, and Zabel.[30] According to the 3D-ER, Nb is tilted compared to the sapphire surface by forming a coherent step pattern. The tilt of the Nb is along one of its [110] axis which is parallel to the $[1\bar{1}01]$ sapphire axis. Assuming no sapphire miscut and monoatomic steps, the width of the Nb terraces can be calculated from this tilt to be about 34 Å. In the case that the sapphire substrate has a certain miscut, the tilt of Nb compared to the physical surface (total tilt) does not agree with the relative tilt between both materials. Instead, the total Nb tilt is determined by the sum of the sapphire miscut and the relative Nb tilt, which may furthermore vary with the in-plane angle. In Fig. 1 we show the situation for the different tilt angles of a sample consisting of an Fe/Cr superlattice, which was deposited on $Cr(001)/Nb(001)/Al_2O_3(1\bar{1}02)$. The angular dependencies of the sapphire miscut and the total tilts of Nb and Fe/Cr were determined from the comparison of the orientations of

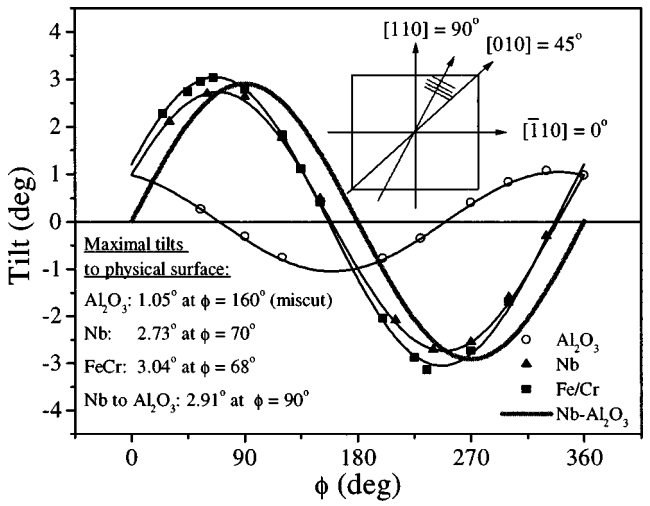

FIG. 1. Measurements of the sapphire miscut and the Nb and Fe/Cr tilts. The measurements have been performed on a superlattice with 200 periods of [(20 Å Fe)/(40 Å Cr)] by low- and high-angle x-ray scattering. The buffers are 120 Å Cr and 500 Å Nb. From the Nb tilt and the sapphire miscut, the relative tilt between both materials was determined.

the x-ray low-angle specular beam to the maxima of the rocking curves in high-angle x-ray diffraction. Subtracting the angular dependence of the sapphire miscut from the total Nb tilt gives the relative Nb tilt. This curve shows a maximum of 2.9° at the Nb[110] orientation, which nicely agrees with the expected behavior from the 3D-ER. However, due to the sapphire miscut angle the total tilt of Nb is rotated away from Nb[110] by about 20°. Due to the epitaxy of Fe/Cr on Nb(001) (see below), Fe and Cr show the same tilt orientations as Nb.

On top of the Nb(001) buffer film a second buffer layer, Cr(001), was grown via effusion cell evaporation with a substrate temperature of 450 °C. For a crucible material we used pyrolytic graphite. To improve the crystal quality and to smooth the surface we subsequently annealed the Cr buffer layer at 750 °C. The crystal lattices of Nb and Cr do not match very well. The lattice parameter misfit between both materials is approximately 14%. Nevertheless, Cr(001) grows epitaxially on Nb(001). As a result of the high lattice misfit the crystal quality of the first monolayers is not very high, but improves with increasing film thickness. We determined that a minimal thickness of the Cr buffer layer of 200 Å is necessary for a sufficiently high film quality. Because of the high crucible volume (39 cm^3) the deposition rate is very stable and reaches a typical value of 0.16 Å/s at 1365 °C at the sample position. The in-plane epitaxial relationship between Cr(001), Nb(001), and $Al_2O_3(1102)$ has been determined by means of grazing incidence x-ray scattering (see Fig. 2). Cr(001) grows nearly parallel to Nb(001). The tilt between Cr(001) and $Al_2O_3(1102)$ is slightly higher as for Nb(001) and $Al_2O_3(1102)$ (see Fig. 1). A similar result was reported earlier by Di Nunzio, Theis-Bröhl, and Zabel.[30] From the tilt of Cr to the sapphire surface an averaged terrace width of about 25 Å can be calculated assuming monoatomic steps.

However, the existence of larger Cr terraces can be assumed for our films. This assumption is supported by *ex situ*

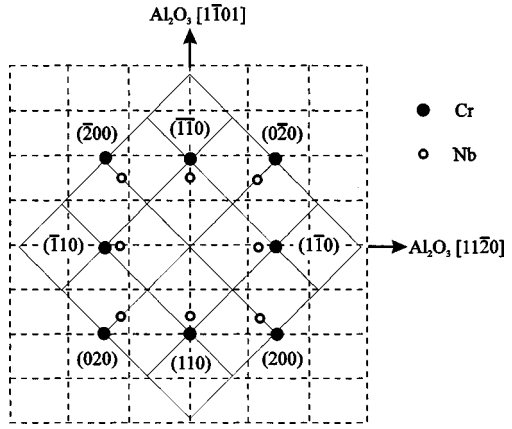

FIG. 2. Epitaxial relations between the sapphire($1\bar{1}02$) plane, Nb(001), and Fe/Cr(001). The measurements were performed via grazing incidence x-ray scattering.

STM measurements (see STM picture in Fig. 3). The STM measurements were performed on a 250-Å-thick Cr film. From a line scan (also shown in Fig. 3) terrace widths of $\approx$200 Å and step heights of $\approx$10–20 Å were observed.

Finally, Fe was deposited by electron-beam evaporation using deposition rates between 0.07 and 1.2 Å/s. Both materials, Fe and Cr, are very well lattice matched (the lattice mismatch is 0.3%) and a sufficiently high film quality was found for substrate temperatures above 100 °C. Because of the anticipated alloying at the Fe/Cr interface for high temperatures the temperature range was limited to 300 °C. For *ex situ* surface protection against oxidation, finally most of the samples were capped with a thin Cr layer.[32]

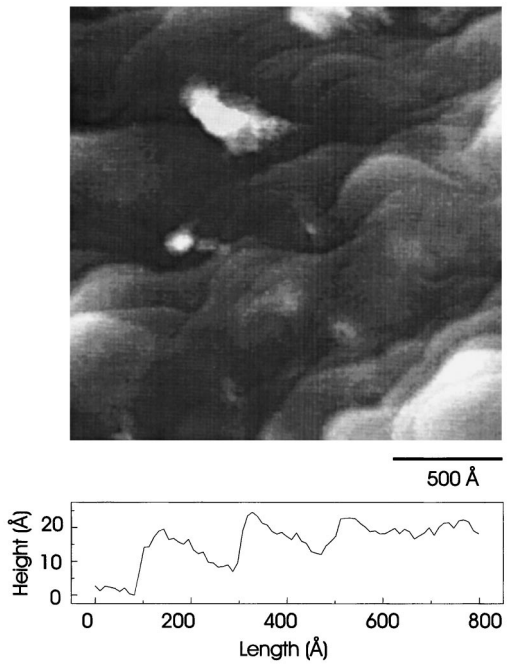

FIG. 3. STM measurement on a sample with 250 Å Cr on 250 Å Nb/Al_2O_3($1\bar{1}02$). The Cr layer was covered with 1–2 ML of Pd to protect it from oxidation. Then, the sample was transferred through air and introduced to an STM. Top: a STM picture in the range 2000 Å$\times$2000 Å is shown. Bottom: a line scan across the terraces is presented.

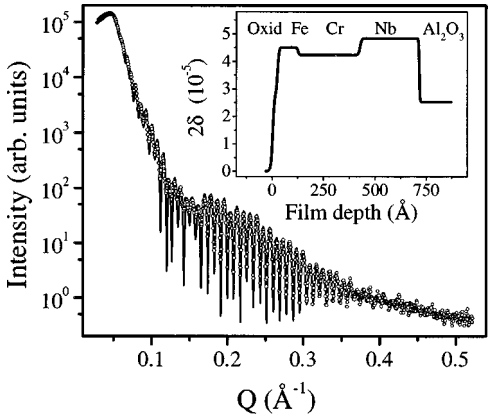

FIG. 4. Small angle x-ray scan for a sample with an Fe thickness of 100 Å, which was evaporated at a growth rate of 0.07 Å/s and a substrate temperature of $T=300$ °C. Inset: Profile of the electron density over the sample that is a result of the fit.

Subsequent to the *in situ* growth studies via RHEED, we measured the thickness and the film quality *ex situ* by high-resolution x-ray scattering. Figure 4 shows a typical small angle x-ray scan for a sample with an Fe thickness of 100 Å, which was evaporated using a growth rate of 0.07 Å/s and a substrate temperature of 300 °C. The individual film thicknesses and the interface roughnesses were calculated by fitting the x-ray data via the Parratt formalism.[33] The result of the fit is illustrated as the solid line in Fig. 4. The inset to Fig. 4 shows the electron density profile along the sample film normal, which is derived from the fit. The results for the interface roughnesses are listed in Table I.

III. *IN SITU* RHEED MEASUREMENTS

We measured RHEED intensity oscillations during the Fe film growth using a 50-kV RHEED gun (data were collected at 30 kV). In our experimental setup the angle of the incident electron beam can be varied in the range from about 1 to 3°. For measuring RHEED intensity oscillations we used the lowest possible angle of incidence, which was determined to be slightly below 1°. With a charge-coupled-device (CCD) camera we monitored the intensity of the complete (00) streak during the Fe film growth. Subsequently, we analyzed the integrated streak intensity within a small window as a function of the growth time t. The lateral window width was chosen such that the specular reflected beam exactly fits into it. In the longitudinal direction we arranged up to 10 windows covering the (00) streak.

For analyzing the RHEED intensity oscillations we directed the e^- beam of the RHEED gun along the Fe[100]

TABLE I. Results of the fits of the x-ray data of an Fe film grown at 300 °C with a rate of 0.07 Å/s.

Material	Thickness	Roughness
Sapphire substrate		3 Å
Nb buffer	289 Å	6 Å
Cr buffer	301 Å	5 Å
Fe film	100 Å	5 Å
Fe-Oxid	24 Å	7 Å

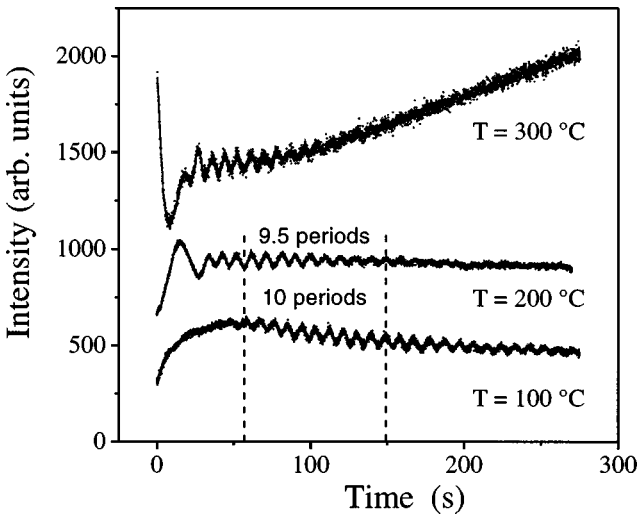

FIG. 5. RHEED intensity oscillations for different substrate temperatures at a growth rate of 0.15 Å/s.

azimuth. In order to eliminate any magnetic influence from the electron-beam evaporator on the RHEED measurements we used high sweeping frequencies of the electron beam; consequently we obtained larger streak widths. Additionally, the noise of the measured intensity increased. Subsequent filtering of the data with a Sawitzky-Golay smoothing algorithm[34] clearly reduced the undesirable noise of the data. By using this algorithm the high frequencies in the measuring signal become damped out without disturbing the amplitudes of the low-frequency parts.

We measured the RHEED intensity in a temperature range between $T=100\,^{\circ}\mathrm{C}$ and $300\,^{\circ}\mathrm{C}$ and at growth rates between $\alpha=0.07$ and 1.2 Å/s. At room temperature, RHEED intensity oscillations could not be found. This indicates that no layer-by-layer growth, but rather 3D island growth occurs at this temperature. Therefore we performed our studies at substrate temperatures of $100\,^{\circ}\mathrm{C}$ and higher. At a temperature of $100\,^{\circ}\mathrm{C}$ and a growth rate of $\alpha=0.35$ Å/s we could identify the maximum of 40 oscillations. Comparing this number of RHEED oscillations with the number of Fe monolayers determined by our x-ray reflectivity measurements, agreement within 1% was obtained, suggesting that one RHEED intensity oscillation period corresponds to the growth of one Fe monolayer.

In Fig. 5 we show RHEED intensity oscillations measured at three different temperatures and with a constant growth rate of $\alpha=0.15$ Å/s. Surprisingly, the largest number of oscillations was observed at the lowest growth temperature. During the early growth stage of the first 2–5 ML of the Fe film growth we could not detect clear RHEED oscillations. This effect is strongly temperature dependent. RHEED oscillations can already be observed at an earlier growth stage at higher temperatures. The reason for this behavior is not completely understood. Alloying may be excluded as a reason for the loss of oscillations, because interface alloying is expected to be small for Fe on Cr as result of the small cohesive energy.[35] Possibly, the growth mode for Fe on Cr differs from the growth mode for Fe on Fe. In contrast to the periodic RHEED intensity oscillations for the early growth, the long term behavior of the RHEED intensity does not exhibit a systematic behavior (see Fig. 5). Sometimes the average

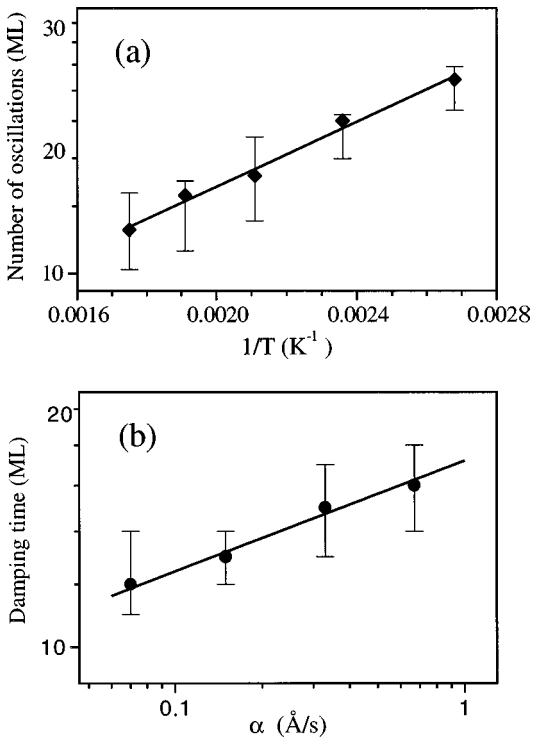

FIG. 6. Arrhenius plot of the observed RHEED oscillations as a function of substrate temperature measured at a constant growth rate of 0.15 Å/s. (a) Double logarithmic plot of the time until RHEED oscillations are fully damped as a function of the growth rate measured at a constant growth temperature of 100 °C (b).

intensity drastically drops after starting the Fe growth and increases again for higher Fe thicknesses. In other cases, the average intensity increases first and later drops. The different behavior may be connected to the relative sample position of the growing film with respect to the e^- beam of the RHEED gun.

We analyzed the RHEED intensity measurements by counting the number n of the observed RHEED oscillations. The results for a constant growth rate of 0.15 Å/s are plotted as a function of the inverse substrate temperature T in an Arrhenius-like plot [see Fig. 6(a)]. The solid line shows a fit to the data points via the expression

$$\ln(n)=-\frac{A}{T}, \tag{1}$$

where $A=-970\pm250$ K. We will discuss these results further below. For the measurements at a constant substrate temperature we analyzed the time t_c for the RHEED oscillation to be fully damped and plotted this time as function of the growth rate α in a log-log plot [see Fig. 6 (b)]. Again we fitted the data by a linear regression and obtained the following relation:

$$\ln(t_c)=-B\,\ln\,\alpha, \tag{2}$$

with $B=-0.14\pm0.11$ Å/s. The relatively large error bars arise from the uncertainty in determining the maximum number of oscillations and the time until oscillations can be observed due to a small signal-to-noise ratio for higher film thicknesses.

Both experiments show that the characteristic damping time t of the RHEED oscillations (which is equivalent to the number of observed RHEED oscillations, n, in constant rate mode) increases with increasing growth rate α or with decreasing substrate temperature T.

IV. GROWTH MODES

Depending on the growth mode, continuum equations can be used to relate the persistence of the oscillations to the growth parameters. In the case of growth on a perfectly flat surface without Ehrlich-Schwoebel barriers,[36] where the kinetic roughening of the surface[37] limits the oscillations, a power law for the damping time t_c of the following form is predicted:[38]

$$\frac{t_c}{\tau} \sim \left(\frac{D a_\perp}{\alpha a^2} \right)^{\delta}. \tag{3}$$

Here τ is the layer completion time (and thus t_c/τ equals the number of visible oscillations n) with $\tau = a_\perp/\alpha$, $a_\perp$ and a being the vertical and lateral lattice constant, respectively. For the surface diffusion constant D an Arrhenius-type behavior,

$$D = a^2 k_0 \exp\left(-\frac{E_a}{k_B T} \right), \tag{4}$$

is assumed, where k_0 is the attempt frequency (typically of the order of $10^{13}\ \mathrm{s}^{-1}$) and E_a is the energy barrier for a diffusion step. Using this expression the dependence of the damping time on the substrate temperature and growth rate can be expressed by

$$\ln(n) = \ln\left(\frac{t_c}{\tau} \right) = -\delta \left(\frac{E_a}{k_B T} + \ln\left(\frac{\alpha}{k_0 a_\perp} \right) \right) + \text{const.} \tag{5}$$

From this, straight lines should be found in an Arrhenius plot of $\ln(t_c)$ versus $1/T$ for a constant growth rate α, and of $\ln(t_c)$ versus $\ln(\alpha)$ for a constant growth temperature T. From the slope of the lines a conclusion about the growth behavior should be possible. As mentioned above, in the absence of Ehrlich-Schwoebel barriers a positive exponent δ is predicted, and was confirmed by computer simulations.[38] This means that an improvement of the layer-by-layer growth is expected with increasing substrate temperature or decreasing growth rate.

Analyzing the Arrhenius plots of our experiments a linear dependence of $\ln(n)$ on $1/T$ (in the case of a constant growth rate α) as well as a linear dependence of $\ln(t_c)$ on $\ln(\alpha)$ (in the case of a constant substrate temperature T) was found [see Figs. 6(a) and 6(b)]. These functional dependencies agree with the results of the theory.[38] However, we observe a negative δ, instead of the expected positive exponent. In the case of Ehrlich-Schwoebel barriers we expect 3D island growth, which leads to an increase of surface roughness with increasing substrate temperature. Numerical simulations were carried out by Siegert and Plischke[39] who find pyramid-like structures on surfaces with Ehrlich-Schwoebel barriers.

In our case [Fe on vicinal Cr(001)], the structural information from RHEED (see Fig. 7) and x-ray diffraction experiments do not indicate stronger surface roughness with increasing substrate temperature. On the contrary, we clearly observe a higher crystal quality and less surface roughness at higher growth temperatures and lower growth rates. This rules out the presence of 3D island growth and another damping mechanism has to be considered.

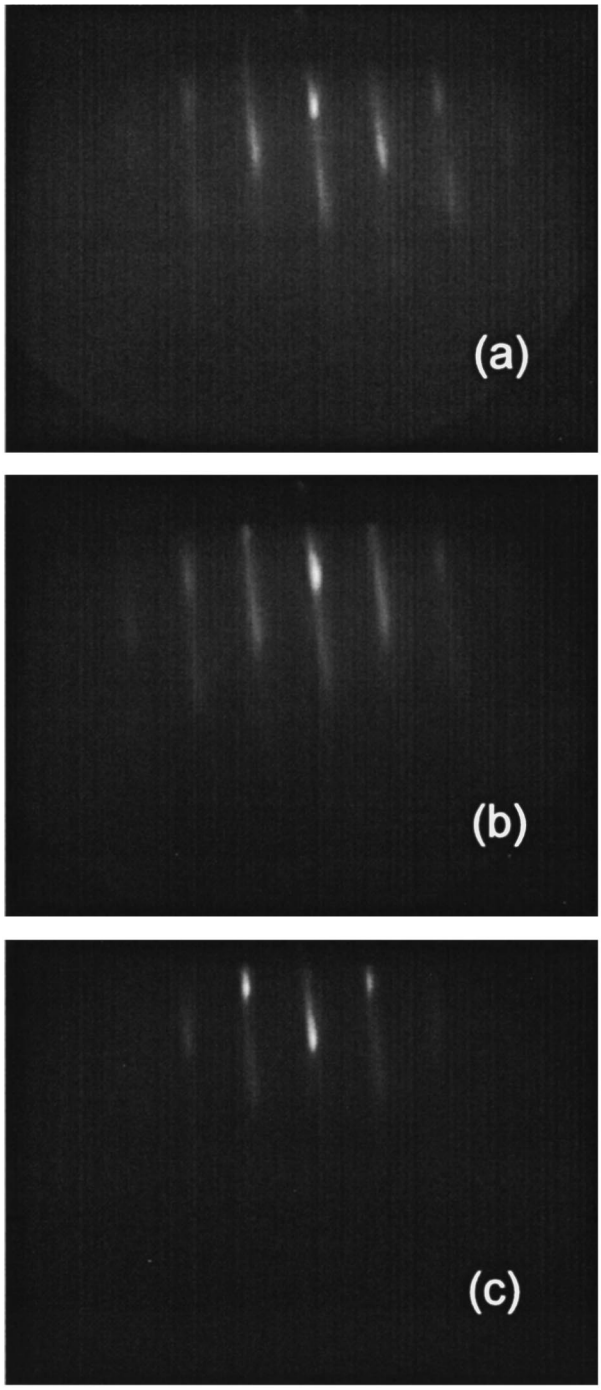

FIG. 7. RHEED patterns of 20-Å-thick Fe(001) films grown on (250 Å Cr)/(500 Å Nb)/Al_2O_3(1102) and taken at three different temperatures [100 °C (a), 200 °C (b), and 300 °C (c)]. The e^- beam was aligned with its azimuth along Fe[100].

Clearly, a vicinal surface with step widths smaller than the typical island distance (on a flat surface) would not lead to any RHEED oscillations. In this case the step density remains essentially constant. This is because almost any atom that lands on the surface is able to diffuse to the step edge

before it can create an island nucleus by encountering another adatom. Thus, the growth mode is not layer-by-layer growth, but step flow, which is stabililized in the presence of Ehrlich-Schwoebel barriers.

This scenario could be present in our system if we had monoatomic steps in the Cr buffer and an average step width of ≈ 25 Å (estimated, using information about the Cr tilt, discussed above). However, the fact that RHEED oscillations are visible at all growth temperatures between 100 and 300 °C contradicts the assumption of a step-flow growth process.

Furthermore, from STM measurements we found terraces of the Cr buffer with step heights larger than 1 ML and widths greater than 25 Å. In such a case, having the same global tilt and having steps that are much higher than one lattice constant or if there are many adjacent steps (step bunch) the situation can be different from that with monoatomic steps. For instance, wide steps allow the nucleation of islands and hence layer-by-layer growth can take place (3D island growth behavior was excluded for our case). Furthermore, in the presence of Ehrlich-Schwoebel barriers the step bunch would not be stable but would dissolve into an essentially regular step train. Recent scaling theory[40] predicts a negative exponent δ for such a scenario.

V. NUMERICAL GROWTH MODEL

We performed computer simulations in which the possible change of growth mode from layer-by-layer growth to step flow during the Fe film growth is mimicked by the dissolution of one high step (several lattice constants). The growth on a tilted surface with initial step bunching is modeled using Monte Carlo simulations based on a well-established solid-on-solid model, in which neither vacancies nor overhangs are allowed.[41]

The crystalline film is treated as a simple cubic lattice. Two processes take place on the surface during growth. First, deposition of atoms occurs, due to a particle flux F. A surface site, on which the particle lands, is chosen randomly. Second, surface diffusion is initiated by lattice vibrations at a substrate temperature T. The diffusion events are modeled as nearest-neighbor hopping processes. The hopping rate is assumed to be

$$k(E,T)=k_0 \exp\left(-\frac{E_a}{k_B T}\right), \tag{6}$$

with the attempt frequency k_0 for hopping processes. The diffusion barrier E_a is comprised of a substrate term E_s, a nearest-neighbor contribution mE_n, m being the number of in-plane nearest neighbors, and an additional contribution E_b due to the Ehrlich-Schwoebel barrier.[36] The latter is realized by assigning to a site a energy penalty proportional to its number of missing out-of-plane next-nearest neighbors. Technically this is done by counting the number of next-nearest neighbors in the planes beneath and above the hopping atom before (m_i) and after (m_f) a hop. The barrier has a nonzero value $(m_i-m_f)E_b$ only if $m_f<m_i$. Note that with this method, an adatom is not directly hindered from hopping down the step but already from approaching it (cf. Ref. 42).

Then the total energy barrier can be written as

$$E_a=E_s+mE_n+(m_f-m_i)E_b\Theta(m_i-m_f), \tag{7}$$

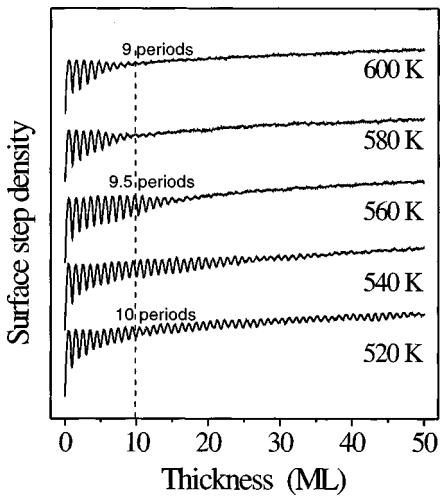

FIG. 8. Results of numerical simulations for the expected dependence of the damping time of RHEED intensity oscillations on the substrate temperature.

with the theta function $\Theta(x)$ having the value one for positive arguments and zero otherwise.

Simulations were carried out on 100×50 lattices. A tilted surface can be easily implemented by periodic boundary conditions. In our simulations the tilt was chosen to be 4% in the direction of the x axis. The surface was initially flat, except for a step bunch comprising four steps. The flux F of the incoming beam adjusted to one particle per second and lattice site, and the energies we used were $E_s=E_n=0.7$ eV and $E_b=0.07$ eV. The temperature T varied between 520 and 600 K.

During the growth of 50 ML the surface step density, which is thought to be proportional to the amount of diffuse reflected RHEED intensity,[43] was monitored continuously. The data (see Fig. 8) clearly show that the growth oscillations persist longer at lower temperatures.

We explain this by the argument already given in the last section: the existence of Ehrlich-Schwoebel barriers stabilizes step flow. So we expect the initial step bunch to dissolve into four separate steps during growth, which are slower the ''colder'' the substrate is. This result of our numerical simulations is illustrated Fig. 9. Snap shots after different growth stages and for two different substrate temperatures show that the dissolution of the step bunch is strongly temperature dependent and happens much faster at the higher temperature. After the dissolution of the step bunch the terraces grow by propagation of steps. This directly translates into a vanishing of oscillations of the step density and the RHEED-reflection intensity (see Fig. 8).

Another effect (though small) can be seen in Fig. 8: the frequency of the oscillations decreases with increasing temperature. For example, its change from $T=520$ K to $T=620$ K amounts to roughly -5%. This is illustrated in Fig. 8 by a decreasing number of periods with increasing temperature during a certain damping time (from 10 periods at 520 K to 9 periods at 600 K). This effect is known in the context of step-flow growth as ''first maximum delay''[44,45] and has its origin in the property of the steps to act as permanent sinks: due to incorporation, adatoms give rise to the step's movement instead of taking part in the nucleation phase. This

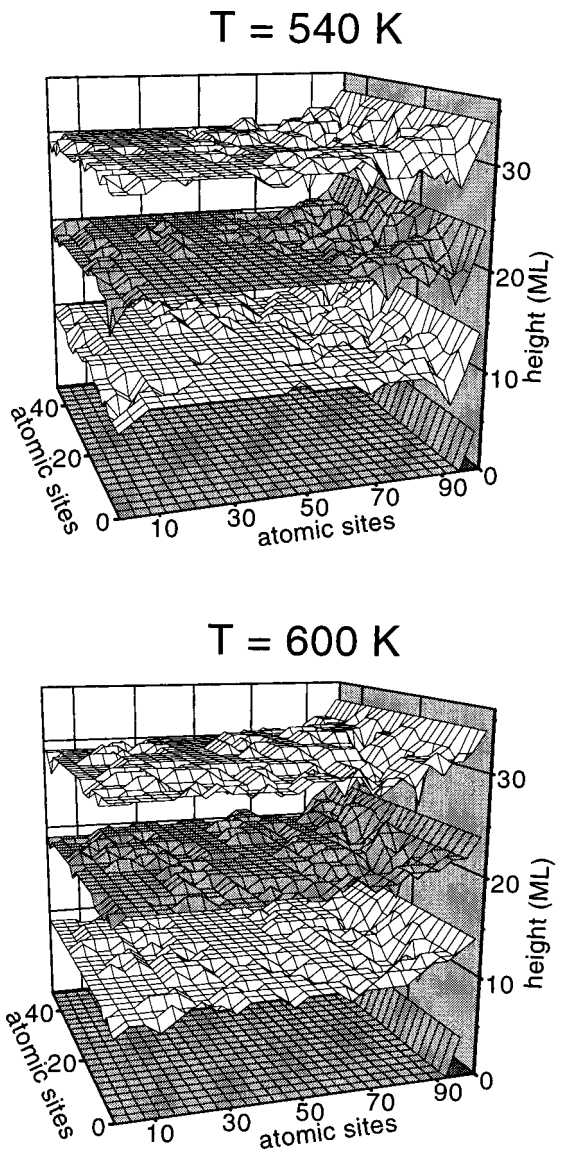

FIG. 9. Illustration of the results of the numerical modulation of the dissolution of a step bunch during the Fe film growth. The picture shows different snapshots (after 0, 10, 20, and 30 ML of Fe growth) for the time dependence of the dissolution of the step bunch at two different substrate temperatures.

affects mainly the islands close to the step and hence has a stronger effect for larger island distances, which are obtained for higher temperatures.[46–48] In our case, the effect is rather weak, since only the lowest step of the bunch ''competes'' with a large terrace.

In the experiments (cf. Fig. 5), the same weak effect can be observed when comparing the curves for $T=100\,^{\circ}\mathrm{C}$ (10 periods during 92 s) and $T=200\,^{\circ}\mathrm{C}$ (9.5 periods during 92 s) (for $T=300\,^{\circ}\mathrm{C}$ the growth conditions seem to be slightly different).

VI. DISCUSSION

The numerical simulations verify our assumption about the Fe growth mode changing from layer-to-layer growth to step flow with increasing temperature. In the present studies the heteroepitaxial Fe growth starts from a vicinal Cr(001) surface having a tilt to the physical surface of $\approx 3°$. The origin of the tilt is the special growth behavior of the particular buffer/substrate system $Nb(001)/Al_2O_3$, which was used for the present experiments (see Sec. II). Following the *ex situ* STM measurements on 250-Å-thick Cr buffers this tilt results in $\approx$200-Å-wide terraces at the Cr surface. The step heights are in the range of $\approx 7-14$ monoatomic steps (see Fig. 3). The precise numbers for the step widths and heights may change for different samples and also for other Nb and Cr buffer thicknesses than the used ones. However, the principal surface morphology of the Cr(001) surface with wide terraces and with steps significantly higher than one monoatomic step will be kept.

For the numerical simulations we assumed a step bunch height of 4 monoatomic steps. This number is smaller than the experimentally observed step height; however, it should be high enough for demonstrating the principal growth behavior. The energy barriers E_s (substrate term) and E_n (nearest-neighbor term) and the additional contribution E_b due to the Ehrlich-Schwoebel barrier were chosen to be close to previous results.[49]

Previous numerical simulations by Siegert and Plischke[39] assuming the existence of Ehrlich-Schwoebel barriers but no vicinal surface result in pyramidlike structures for the growing film. The growth mode changes from layer-by-layer to 3D island growth in this case, which leads to an increase of surface roughness with increasing substrate temperature. The situation changes for the growth on a vicinal surface. In this case, Ehrlich-Schwoebel barriers result in step-flow growth.

In the present case (wide terraces and steps higher than one monoatomic step) the terrace width is too wide for a perfect step-flow behavior. In the beginning of the Fe growth only a few atoms are able to diffuse to the step edges. Atoms that land at large distances from the step edges are not able to reach them before encountering other adatoms and creating an island. Therefore, predominantly layer-by-layer growth is observed in the beginning of the Fe growth. The numerical simulations show that the previous step bunches are not stable but dissolve into a regular step train during the Fe growth. This leads to a decreasing terrace width with increasing Fe film thickness and the step-flow growth mode more and more dominates the growth behavior. This process is temperature dependent. The higher diffusivity of the Fe particles at higher temperatures increases the chance to reach the step edge instead of creating an island with another adatom. This results in a higher velocity of the steps and hence in a faster dissolution of the step bunch. Therefore, the RHEED oscillations are damped out faster (at fixed growth rate). In the case of a fixed temperature the chance of island nucleation is lowered with decreasing growth rate, resulting again in a faster (in relation to the growing velocity) movement of the steps.

The dissolution of the steps during the Fe film growth can be considered as a melting process. To verify this behavior *in situ* STM studies during the Fe film growth should be performed. The preliminary *ex situ* STM measurements on a Cr buffer (Fig. 3) verify the existence of step bunches in the beginning of the Fe growth.

We now discuss our results with respect to the magnetic properties of the Fe/Cr system. In the Introduction we pointed out the interrelationship between interface morphol-

ogy and magnetic properties in the Fe/Cr system. The steps at the Fe/Cr interfaces will influence the magnetic properties and will cause spin frustration effects in the Cr spacers. The magnetic structure of the Cr spacer layers in Fe/Cr superlattices on $Cr/Nb/Al_2O_3$ was studied recently by Schreyer *et al.*[15] The results of this study qualitatively agree with theoretical predictions for fluctuating Cr thicknesses[12] originated by steps at the Fe/Cr interface. A quantitative relation between the step density and the step height has yet to be made. For other systems [such as the growth of Fe/Cr on Ag buffer using Fe-covered GaAs as substrate,[10] and for the growth of Fe/Cr on MgO (Refs. 13 and 50)] other morphologies of the Cr/Fe interfaces may be expected and therefore different step densities and step heights will be present. To compare results for the coupling behavior across the Cr spacer and the spin state of Cr, surface morphology studies of the interface between Fe and Cr are necessary. This has been done in a few cases, for instance, by the means of STM studies for the system Fe/Cr on Ag (using GaAs as substrate) (Ref. 51) and on Fe whiskers.[52]

VII. SUMMARY

We have studied RHEED intensity oscillations during the Fe(001) growth on vicinal $Cr/Nb/Al_2O_3$ at different growth temperatures and growth rates. The logarithm of the number of RHEED oscillations shows a linear dependence on the inverse growth temperature. Similarly, a straight line was found in a double logarithmic plot for damping time versus growth rate. This result seems to agree with the theory describing growth without Ehrlich-Schwoebel barriers. However, in our case the slope of the straight lines has a negative sign in contrast to a positive one predicted by the theory. We explain the Fe growth behavior by melting of previously existing step bunches (in the Cr buffer layer). This assumption was verified by numerical simulations. For the Cr-buffer terraces up to 200 Å wide and having steps several monolayers high can be inferred from *ex situ* STM measurements. This result supports our interpretation for the Fe growth behavior because it verifies the existence of step bunches in Cr.

ACKNOWLEDGMENTS

The authors wish to acknowledge technical support by J. Podschwadek and C. Leschke. Thanks go also to G. Wilhelmi for performing the STM measurements and A. Schreyer for fruitful discussions. This work was supported by the Deutsche Forschungsgemeinschaft through SFB 166.

[1] P. Grünberg, R. Schreiber, Y. Pang, M. B. Brodsky, and H. Sowers, Phys. Rev. Lett. **57**, 2442 (1986).

[2] S. S. P. Parkin, N. More, and K. P. Roche, Phys. Rev. Lett. **64**, 2304 (1990).

[3] S. Demokritov, J. A. Wolf, and P. Grünberg, Europhys. Lett. **15**, 881 (1991).

[4] J. Unguris, R. J. Celotta, and D. T. Pierce, Phys. Rev. Lett. **67**, 140 (1991); **69**, 1125 (1992).

[5] S. T. Purcell, W. Folkerts, M. T. Johnson, N. W. E. McGee, K. Jager, J. aan de Stegge, W. B. Zeper, W. Hoving, and P. Grünberg, Phys. Rev. Lett. **67**, 903 (1991).

[6] M. N. Baibich, J. M. Broto, A. Fert, F. Nguyen van Dau, F. Petroff, P. Etienne, G. Creuzet, A. Friederich, and J. Chazelas, Phys. Rev. Lett. **61**, 2472 (1988).

[7] G. Binasch, P. Grünberg, F. Saurenbach, and W. Zinn, Phys. Rev. B **39**, 4828 (1989).

[8] P. Bruno and C. Chappert, Phys. Rev. Lett. **67**, 1602 (1991).

[9] B. Heinrich and J. F. Cochran, Adv. Phys. **42**, 523 (1993).

[10] J. A. Wolf, Q. Leng, R. Schreiber, P. A. Grünberg, and W. Zinn, J. Magn. Magn. Mater. **121**, 253 (1993).

[11] M. Rührig, R. Schäfer, A. Hubert, R. Mosler, J. A. Wolf, S. Demokritov, and P. Grünberg, Phys. Status Solidi A **125**, 635 (1991).

[12] J. C. Slonczewski, J. Magn. Magn. Mater. **150**, 13 (1995).

[13] E. F. Fullerton, K. T. Riggs, C. H. Sowers, A. Berger and S. D. Bader, *Magnetic Ultrathin Films, Multilayers and Surfaces*, edited by A. Fert *et al.*, MRS Symposia Proc. No. 384 (Materials Research Society, Pittsburgh, 1995), p. 145.

[14] D. Stoeffler and F. Gautier, in *Magnetism and Structure in Systems of reduced Dimensions*, edited by B. Dieny, R. F. C. Farrow, M. Donath, A. Fert, and B. D. Hermsmeier (Plenum Press, New York, 1993), p. 411; D. Stoeffler and F. Gautier, Phys. Rev. B **44**, 10 389 (1991); A. Vega, D. Stoeffler, H. Dreyssé, and C. Demangeat, Europhys. Lett. **31**, 561 (1995).

[15] A. Schreyer, C. F. Majkrzak, Th. Zeidler, T. Schmitte, P. Bödeker, K. Theis-Bröhl, A. Abromeit, J. Dura, and T. Watanabe, Phys. Rev. Lett. **79**, 4914 (1997).

[16] See, for example, *Reflection High Energy Electron Diffraction and Reflection Electron Imaging on Surfaces*, Vol. 188 of *NATO Advanced Studies Institute Series B: Physics*, edited by P. K. Larson and P. J. Dobson (Plenum, New York, 1988).

[17] J. J. Harris, B. A. Joyse, and P. J. Dobson, Surf. Sci. **103**, L190 (1981); **108**, L444 (1981).

[18] C. E. C. Wood, Surf. Sci. **108**, L441 (1981).

[19] T. Kaneko, M. Imafuku, C. Kokubu, R. Yamamoto, and M. Doyama, J. Phys. Soc. Jpn. **55**, 2903 (1986).

[20] S. T. Purcell, B. Heinrich, and A. S. Arrott, Phys. Rev. B **35**, 6458 (1987).

[21] C. Koziol, G. Lienkamp, and E. Bauer, Appl. Phys. Lett. **51**, 901 (1987).

[22] L. M. Peng and M. J. Whelan, Surf. Sci. **238**, L446 (1990).

[23] J. A. Stroscio, D. T. Pierce, and R. A. Dragoset, Phys. Rev. Lett. **70**, 3615 (1993).

[24] A. Schatz, S. Dunkhorst, S. Lingnau, U. von Hörsten, and W. Keune, Surf. Sci. **310**, L595 (1994).

[25] K. Theis-Bröhl, R. Scheidt, Th. Zeidler, F. Schreiber, H. Zabel, Th. Mathieu, C. Mathieu, and B. Hillebrands, Phys. Rev. B **53**, 11 613 (1996).

[26] S. M. Durbin, J. E. Cunningham, and C. P. Flynn, J. Phys. F **12**, L75 (1982).

[27] K. Bröhl, P. Bödeker, A. Stierle, and H. Zabel, J. Cryst. Growth **127**, 682 (1993).

[28] J. Mayer, C. P. Flynn, and M. Rühle, Ultramicroscopy **33**, 51 (1990).

[29] G. Gutekunst, J. Mayer, and M. Rühle, Phylosoph. Magazin. A **75**, 1329 (1997); **75**, 1357 (1997).
[30] S. Di Nunzio, K. Theis-Bröhl, and H. Zabel, Thin Solid Films **279**, 180 (1996).
[31] K. M. Knowles, K. B. Alexander, R. E. Somekh, and W. M. Stobbs, *Electron Microscopy and Analysis*, 1987, edited by M. L. Brown, IOP Conf. Proc. No. 90 (Institute of Physics, Bristol, 1987), p. 245.
[32] A. Stierle, P. Bödeker, and H. Zabel, Surf. Sci. **327**, 9 (1995); A. Stierle and H. Zabel, Europhys. Lett. **37**, 365 (1997).
[33] L. G. Parratt, Phys. Rev. **95**, 359 (1954).
[34] Described in W. H. Press, S. A. Teukolsky, W. T. Vetterling, and B. P. Flannery, *Numerical Recipes in C* (Cambridge University Press, Cambridge, 1992).
[35] B. Heinrich *et al.*, J. Appl. Phys. **81**, 4350 (1997).
[36] G. Ehrlich and F. G. Hudda, J. Chem. Phys. **44**, 1039 (1966); R. L. Schwoebel and E. J. Shipsley, J. Appl. Phys. **37**, 3682 (1966); R. L. Schwoebel, *ibid.* **40**, 614 (1968); S. Wang and G. Ehrlich, Phys. Rev. Lett. **70**, 41 (1992).
[37] J. Krug and H. Spohn, in *Solids Far From Equilibrium: Growth, Morphology and Defects*, edited by C. Godrèche (Cambridge University Press, Cambridge, 1990).
[38] H. Kallabis, L. Brendel, J. Krug, and D. E. Wolf, Int. J. Mod. Phys. B **1997**, 77.
[39] M. Siegert and M. Plischke, Phys. Rev. Lett. **73**, 1517 (1994); M. Siegert and M. Plischke, Phys. Rev. E **50**, 917 (1994).
[40] L. Brendel and D. E. Wolf (unpublished).
[41] P. Šmilauer and D. D. Vvedensky, Phys. Rev. B **52**, 14 263 (1995).
[42] P. Šmilauer, M. R. Wilby, and D. Vvedensky, Phys. Rev. B **47**, 4119 (1993).
[43] D. E. Wolf, in *Scale Invariance, Interfaces and Non-Equilibrium Dynamics*, edited by A. J. McKane (Plenum, New York, 1994).
[44] H. T. W. Zandvliet, H. B. Elswijk, D. Dijkkamp, E. J. van Loenen, and J. Dieleman, J. Appl. Phys. **70**, 2614 (1991).
[45] T. Shitara, J. Zhang, J. H. Neave, and B. A. Joyce, J. Appl. Phys. **71**, 4299 (1992).
[46] J. A. Venables, G. D. Spiller, and M. Hanbücken, Rep. Prog. Phys. **47**, 399 (1984).
[47] L. H. Tang, J. Phys. I **3**, 935 (1993).
[48] S. Günther, E. Kopatzki, M. C. Bartelt, J. W. Evans, and R. J. Behm, Phys. Rev. Lett. **73**, 553 (1994).
[49] P. Šmilauer and D. D. Vvedensky, Phys. Rev. B **48**, 17 603 (1993).
[50] J. Meersschaut, J. Dekoster, R. Schad, P. Beliën, and M. Rots, Phys. Rev. Lett. **75**, 1638 (1995).
[51] D. E. Bürgler, C. M. Schmidt, J. A. Wolf, T. M. Schaub, and H.-J. Güntherodt, Surf. Sci. **366**, 295 (1996); D. E. Bürgler, C. M. Schmidt, D. M. Schaller, F. Meisinger, R. Hofer, and H.-J. Güntherodt, Phys. Rev. B **56**, 4149 (1997).
[52] A. Davies, J. A. Stroscio, D. T. Pierce, and R. J. Celotta, Phys. Rev. Lett. **76**, 4175 (1996); J. Magn. Magn. Mater. **165**, 82 (1997).